Transmitter-Side Multipath Preprocessing for Pulsed UWB Systems Considering Pulse Overlapping and Narrow-Band Interference

Shiwei Zhao and Huaping Liu, *Member, IEEE*

***Abstract*—We analyze a prerake diversity combining scheme for pulsed ultrawideband systems to shift signal processing needs from the receiver to the transmitter. We consider the realistic case that received pulses carrying the same transmitted symbol could overlap with one another in optimizing the prerake scheme based on zero-forcing and eigenanalysis techniques. We show that in the presence of interpulse interference caused by pulse overlapping, the optimum prerake combining scheme in the sense of maximizing the received signal-to-noise ratio derived by using the eigenanalysis technique performs the same as a conventional rake with maximal ratio combining. We also analyze the different behaviors of prerake and rake schemes in the presence of tone interferers and provide numerical results to validate the conclusions in the presence of in-band-modulated interferers. We find that when the number of narrow-band interference (NBI) signals is small, the prerake scheme outperforms the rake scheme; as the number of NBI sources increases, however, this performance gap reduces.**

***Index Terms*—Interpulse interference, narrow-band interference (NBI), prerake multipath combining, ultrawideband (UWB).**

I. Introduction

ULTRAWIDEBAND (UWB) communications could be achieved using the orthogonal-frequency-division-multiplexing technique [1], [2] or the pulsed technique [3]–[6]. One of the advantages of pulsed UWB communications is its ability to resolve individual multipath components. This requires a rake receiver to gain path diversity and to capture multipath energy.

Multipath combining through a rake [7], [8] requires multipath tracking and channel estimation. However, hardware complexity, power consumption, and system cost scale up significantly with the number of paths combined, which should be avoided for portable or mobile units. Most UWB networks have fixed access points, and it is very desirable if the rake processing can be shifted from the mobile receivers to the transmitter at a fixed access point. As such a shift usually requires channel-state information (CSI) in the transmitter, this technique is attractive for systems with time-division duplexing (TDD), where CSI can easily be obtained at both the transmitter and the receiver since both the uplink and the downlink of TDD systems operate in the same frequency band.

For TDD code-division multiple-access systems, a transmit precoding technique is investigated in [9]. This scheme suggests a prerake structure in which predelayed signal transmission is employed in the transmitter. This scheme is shown to have comparable performances with the common rake receivers. The prerake scheme has recently been applied to pulsed UWB systems [10] in which the ideal case that received adjacent paths are separated in time by at least one pulsewidth is assumed. This assumption might be acceptable for communications in line-of-sight (LOS) environments. In non-LOS indoor environments, however, it becomes inappropriate. For example, the typical average multipath arrival rate is in the range of 0.5–2 ns [11], [12], and the typical pulse duration could be as large as 1–4 ns [13] for pulses with a 10-dB bandwidth of 500 MHz–2 GHz. This could cause severe interpulse interference (IPI). Detection and performance in the presence of IPI are studied in [14]–[16]. Besides IPI due to pulse overlapping, coexisting narrow-band radios will interfere with UWB systems. The effects of narrow-band interference (NBI) to UWB systems with rake reception have been analyzed extensively [17], [18]. Prerake systems are expected to function differently from the conventional rake receiver in the presence of NBI. Therefore, the conclusions made in existing research on prerake UWB systems need to be reexamined, and some optimizations might help to improve performance when pulse overlapping and NBI are taken into consideration. The time-reversal technique, which originated from wideband transmission in underwater acoustics and has recently been applied to UWB communications [19], is also similar to the prerake scheme; however, IPI and NBI are not considered in [19].

In this paper, we study the structure, optimization, and performance of prerake UWB systems when pulse overlapping and NBI are taken into consideration. Background information such as the transmitted signal, the UWB channel model, and the basic prerake scheme will be described in Section II. Section III discusses two different optimization approaches at the transmitter to overcome the interference caused by pulse overlapping. Section IV addresses the effects of NBI. Analytical performance expressions are obtained for an environment

Manuscript received January 15, 2006; revised July 31, 2006, January 12, 2007, and January 16, 2007. The review of this paper was coordinated by Prof. R. M. Buehrer.

S. Zhao was with the School of Electrical Engineering and Computer Science, Oregon State University, Corvallis, OR 97331 USA. He is now with Trapeze Networks, Pleasanton, CA 94588 USA (e-mail: zhao@trapezenetworks.com).

H. Liu is with the School of Electrical Engineering and Computer Science, Oregon State University, Corvallis, OR 97331 USA (e-mail: hliu@eecs.oregonstate.edu).

Color versions of one or more of the figures in this paper are available online at http://ieeexplore.ieee.org.

Digital Object Identifier 10.1109/TVT.2007.901061

with tone interferers to illustrate how NBI affects the performance of rake and prerake systems. Simulation results are provided in Section V to validate the analysis and to compare the performances of different algorithms in the presence of IPI and NBI. The concluding remarks are provided in Section VI.

II. Transmitter-Side Diversity Combining: Prerake Method

A. Transmitted Signal and Channel Model

In pulsed UWB systems with binary pulse-amplitude modulation (PAM), the transmitted signal without prerake processing is expressed as

$$s(t) = \sum_{i=-\infty}^{\infty} s_i(t) = \sum_{i=-\infty}^{\infty} \sqrt{E_{\rm b}} b(i) p(t - iT_{\rm b}) \qquad (1)$$

where $p(t)$ is the short-duration UWB pulse shape of width $T_{\rm p}$, $E_{\rm b}$ is the bit energy, $T_{\rm b}$ is the bit interval ($T_{\rm b} \gg T_{\rm p}$), and $b(i) \in \{1, -1\}$ is the ith information bit. The energy of the basic pulse $p(t)$ is normalized to $E_{\rm p} = \int_{-\infty}^{\infty} p^2(t)dt = 1$. $s(t)$ is then transmitted through a frequency-selective lognormal fading channel [11], [20] with additive white Gaussian noise (AWGN). It is well known that the channel for pulsed UWB systems exhibits highly frequency-selective fading, and it can be modeled as a discrete linear filter with an impulse response

$$h(t) = \sum_{l=0}^{L-1} \alpha_l \delta(t - \tau_l) \qquad (2)$$

where L is the total number of multipath components, α_l is the channel fading coefficient for the lth path, τ_l is the arrival time of the lth path relative to the first path ($\tau_0 = 0$ assumed), and $\delta(t)$ is the Dirac delta function. The channel gain α_l is modeled as $\alpha_l = \lambda_l \beta_l$, where λ_l takes on the values of -1 or 1 with equal probability [11]. Since multipath components tend to arrive in clusters [11], τ_l in (2) is expressed as $\tau_l = \mu_c + \nu_{m,c}$, where μ_c is the delay of the cth cluster in which the lth path falls, and $\nu_{m,c}$ is the delay (relative to μ_c) of the mth multipath component in the cth cluster. The relative power of the lth path to the first path can be expressed as $E\{|\alpha_l|^2\} = E\{|\alpha_0|^2\} e^{-\mu_c/\Gamma} e^{-\nu_{m,c}/\gamma}$, where $E\{\cdot\}$ denotes expectation, Γ is the cluster decay factor, and γ is the ray decay factor. Note that, different from common baseband models of narrow-band systems, α_l is real-valued in the UWB channel model.

B. Prerake Model

The concept of prerake diversity combining has been illustrated in [9] and [10]. For completeness and for the readers' convenience, we summarize the prerake model in this section. We assume that the signaling rate is such that the received signal energy of a particular bit is contained within one pulse repetition interval ($T_{\rm b}$) so that there is no intersymbol interference (ISI). Thus, we can focus on a particular bit interval in the receiver modeling. Corresponding to the signal $s_i(t)$ that carries the ith information bit given in (1), the received signal is expressed as

$$r(t) = \sum_{l=0}^{L-1} \alpha_l s_i(t - \tau_l) + n(t) \qquad (3)$$

where $n(t)$ is the white Gaussian noise process with a two-sided power spectral density of $N_0/2$.

Assuming perfect timing and perfect estimates of channel coefficients and multipath delays, the correlator output of the lth finger in a generic rake receiver that combines the first $L_{\rm p} (L_{\rm p} < L)$ paths is expressed as

$$r_l = \sum_{k=0}^{L_{\rm p}-1} \left(\alpha_k \sqrt{E_{\rm b}} b(i) \int_{-\infty}^{\infty} p(t - iT_{\rm b} - \tau_k) p(t - iT_{\rm b} - \tau_l) dt \right) + n_l, \quad l = 0, 1, \ldots, L_{\rm p} - 1 \qquad (4)$$

where the zero-mean noise component is $n_l = \int_{-\infty}^{\infty} n(t) p(t - iT_{\rm b} - \tau_l) dt$ with variance $\sigma_{n_l}^2 = N_0/2$. When $|\tau_j - \tau_i| < T_{\rm p}$, $i, j \in \{0, 1, \ldots, L-1\}$, the ith and the jth received pulses overlap with each other, causing IPI. For the ideal but nonrealistic case when $|\tau_j - \tau_i| > T_{\rm p}, i, j \in \{0, 1, \ldots, L-1\}$, received pulses do not overlap. In this case, all terms with $k \neq l$ in (4) are equal to zero, and r_l simplifies to

$$r_l = \alpha_l \sqrt{E_{\rm b}} b(i) + n_l, \qquad l = 0, 1, \ldots, L_{\rm p} - 1 \qquad (5)$$

where noise components $n_l, l = 0, \ldots, L_{\rm p} - 1$, are mutually independent.

In rake systems with linear combining, the decision variable is derived based on the outputs of the $L_{\rm p}$ rake fingers. Let $\boldsymbol{r} = [r_0, r_1, \ldots, r_{L_{\rm p}-1}]^{\rm T}$ (superscript $^{\rm T}$ denotes transpose), $\boldsymbol{\alpha} = [\alpha_0, \alpha_1, \ldots, \alpha_{L_{\rm p}-1}]^{\rm T}$, and $\boldsymbol{\omega} = [\omega_0, \omega_1, \ldots, \omega_{L_{\rm p}-1}]^{\rm T}$ be the tap weight vector for linear combining. The decision variable is expressed as $\Delta = \boldsymbol{\omega}^{\rm T} \boldsymbol{r}$. It is well known that maximal ratio combining (MRC) is optimum when the desired signal is distorted only by AWGN. The MRC weights that maximize the output signal-to-noise ratio (SNR) are written as $\boldsymbol{\omega} = \boldsymbol{\alpha}^* = [\alpha_0, \alpha_1, \ldots, \alpha_{L_{\rm p}-1}]^{\rm H}$, where $(\cdot)^*$ denotes complex conjugate, and superscript $^{\rm H}$ denotes Hermitian transpose.

In prerake systems, $L_{\rm p}$ pulses that are each scaled and delayed based on the multipath coefficients and delays are transmitted in each bit interval. The channel acts as a filter. The scaling coefficients and relative delays are controlled such that the output peak of the correlator in the receiver is equivalent to the output of a conventional rake with MRC. This scheme is shown in Fig. 1. Note that, in the prerake system, the receiver requires only one correlator and does not need to perform channel estimation and multipath tracking.

The transmitted signal (again, only the signal in the ith bit interval is modeled) in a prerake system is expressed as

$$s_i'(t) = \sqrt{\frac{1}{\kappa}} \sum_{l=0}^{L_{\rm p}-1} \alpha_{L_{\rm p}-1-l}^* s_i(t + \tau_l) \qquad (6)$$

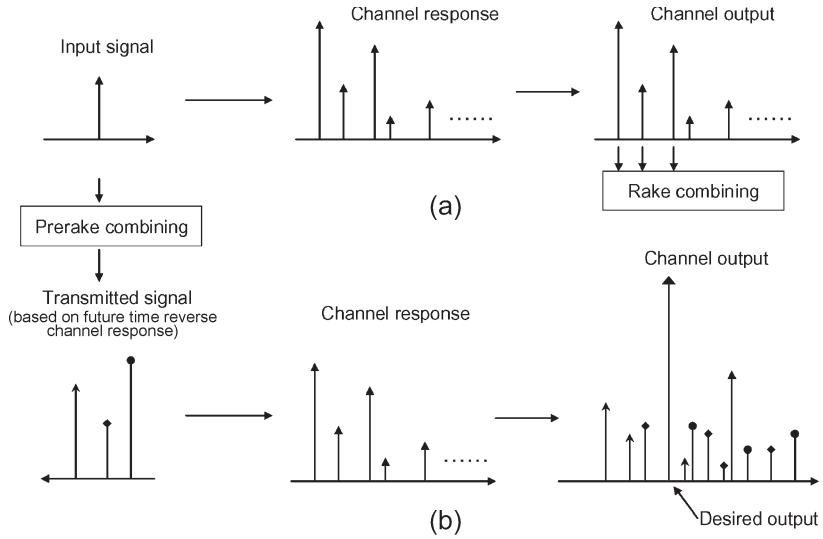

Fig. 1. Rake and prerake systems. (a) Rake diversity combining. (b) Prerake diversity combining.

where $\kappa = \boldsymbol{\alpha}^{\mathrm{H}}\boldsymbol{\alpha}$ is a power normalization factor. After passing through the frequency-selective fading channel described by (2), $s_i'(t)$ arrives at the receiver as

$$r'(t) = \sqrt{\frac{E_{\mathrm{b}}}{\kappa}} b(i) \sum_{l=0}^{L_{\mathrm{p}}-1} \alpha^*_{L_{p-1-l}} \sum_{k=0}^{L-1} \alpha_k p(t - iT_{\mathrm{b}} + \tau_l - \tau_k) + n(t). \tag{7}$$

The receiver uses only the strongest path to detect the ith bit.[1] The correlator output is expressed as

$$\Delta' = \int_{-\infty}^{\infty} r'(t) p(t - iT_{\mathrm{b}}) dt. \tag{8}$$

In the absence of pulse overlapping, ideally, when spaces between all adjacent paths are larger than the UWB pulsewidth T_{p}, Δ' simplifies to

$$\Delta' = \sqrt{\frac{E_{\mathrm{b}}}{\kappa}} b(i) \sum_{l=0}^{L_{\mathrm{p}}-1} \alpha^*_l \alpha_l + n' \tag{9}$$

where the zero-mean noise component $n' = \int_{-\infty}^{\infty} n(t) p(t - iT_{\mathrm{b}}) dt$ has a variance of $N_0/2$.

Let us examine the output SNR of the rake and prerake systems. For the conventional rake system, let $\boldsymbol{n} = [n_0, n_1, \ldots, n_{L_{\mathrm{p}}-1}]^{\mathrm{T}}$ be the noise vector. The instantaneous output SNR of the rake combiner is $\psi = ((\boldsymbol{\alpha}^{\mathrm{H}}\boldsymbol{\alpha})^2 E_{\mathrm{b}})/(2E\{(\boldsymbol{\alpha}^{\mathrm{H}}\boldsymbol{n})^{\mathrm{H}}(\boldsymbol{\alpha}^{\mathrm{H}}\boldsymbol{n})\})$, where $E\{(\boldsymbol{\alpha}^{\mathrm{H}}\boldsymbol{n})^{\mathrm{H}}(\boldsymbol{\alpha}^{\mathrm{H}}\boldsymbol{n})\} = \boldsymbol{\alpha}^{\mathrm{H}}\boldsymbol{\alpha} E\{\boldsymbol{n}^{\mathrm{H}}\boldsymbol{n}\} = \boldsymbol{\alpha}^{\mathrm{H}}\boldsymbol{\alpha} N_0/2$. In the receiver of the prerake system, the output signal energy is $((\boldsymbol{\alpha}^{\mathrm{H}}\boldsymbol{\alpha})^2 E_{\mathrm{b}})/\kappa = (\boldsymbol{\alpha}^{\mathrm{H}}\boldsymbol{\alpha}) E_{\mathrm{b}}$. Since the prerake receiver does not need multipath combining, we have $E\{n'^* n'\} = N_0/2$. Although only the energy of the strongest path is collected, the total noise energy also scales down accordingly. The output SNR of prerake systems is $\psi = E_{\mathrm{b}}(\boldsymbol{\alpha}^{\mathrm{H}}\boldsymbol{\alpha})/N_0$, which is equal to the rake combiner output SNR. Moreover, the diversity orders of the rake and prerake systems are the same. Consequently, both schemes have the same performance, which will be verified by the simulation in Section V.

[1]The L_pth path whose delay is relative to the first-arriving path is τ_{L_p-1} (see Fig. 1).

III. Prerake Optimization in the Presence of Pulse Overlapping

Since pulse overlapping causes IPI, (5) and (9) no longer hold. Following the notation used in [15], we define the partial correlation between $p(t - \tau_k)$ and $p(t - \tau_l)$ as $\rho_{l,k} = \int_{-\infty}^{\infty} p(t - \tau_l) p(t - \tau_k) dt = \rho_{k,l}$. Since the energy of $p(t)$ is normalized to unity, $\rho_{l,k} = 1$ for $l = k$, and $0 \le |\rho_{l,k}| < 1$ for $l \ne k$. Note that $\rho_{l,k} = 0$ if $p(t - \tau_k)$ and $p(t - \tau_l)$ are mutually orthogonal or do not overlap with each other.

For rake receivers derived from the signal model given in (4), the received signal vector becomes

$$\boldsymbol{r} = \sqrt{E_{\mathrm{b}}} b(i) \boldsymbol{R}\boldsymbol{\alpha} + \boldsymbol{n} \tag{10}$$

where

$$\boldsymbol{R} = \begin{bmatrix} 1 & \rho_{0,1} & \cdots & \rho_{0,L_{\mathrm{p}}-1} \\ \rho_{1,0} & 1 & \cdots & \rho_{1,L_{\mathrm{p}}-1} \\ \vdots & \vdots & \ddots & \vdots \\ \rho_{L_{\mathrm{p}}-1,0} & \rho_{L_{\mathrm{p}}-1,1} & \cdots & 1 \end{bmatrix} \tag{11}$$

is the partial correlation matrix, which can be calculated using the relative multipath delays τ_l and the pulse shape $p(t)$. Thus, the zero-mean noise components at the output of different receiver fingers are no longer independent, and the covariance matrix of $\boldsymbol{n}$ (zero mean) is obtained to be $E\{\boldsymbol{n}\boldsymbol{n}^{\mathrm{H}}\} = \boldsymbol{R}(N_0/2)$. The decision variable is still $\Delta = \boldsymbol{\omega}^{\mathrm{T}}\boldsymbol{r}$, where the optimum choice of $\boldsymbol{\omega}$ can be found in [15]. Note that, in the model given by (10) and (11), the effect caused by the potential overlap from paths $L_{\mathrm{p}}, \ldots, L$, whose average power is lower than that of the earlier arriving paths, has been neglected.

As shown in Fig. 1, the nonuniform time intervals between different multipath components could be very small, and the

overlap between multipaths leads to IPI. Because of the additional distortion to the received signals caused by IPI and the noise correlation, prerake schemes designed according to the MRC rule may not be optimum. We define the scaling coefficients expressed in a vector for pulses constituting $s_i'(t)$ in prerake systems as $\boldsymbol{w} = [w_0, w_1, \ldots, w_{L_\mathrm{p}-1}]^\mathrm{T}$. Then, $s_i'(t)$ can be rewritten as

$$s_i'(t) = \sqrt{\frac{1}{\kappa}} \sum_{l=0}^{L_\mathrm{p}-1} w_{L_\mathrm{p}-1-l} s_i(t+\tau_l) \tag{12}$$

where the power normalization factor becomes $\kappa = \boldsymbol{w}^\mathrm{H}\boldsymbol{R}\boldsymbol{w}$. Correspondingly, (9) becomes

$$\Delta' = \sqrt{\frac{E_\mathrm{b}}{\kappa}} b(i)\boldsymbol{w}^\mathrm{T}\boldsymbol{R}\boldsymbol{\alpha} + n'. \tag{13}$$

A. Zero-Forcing (ZF) Optimization

From (13), a natural choice of the prerake weight vector $\boldsymbol{w}$ to overcome the effect of IPI is to apply the ZF scheme, which yields a weight vector

$$\boldsymbol{w}^\mathrm{T} = \boldsymbol{\alpha}^\mathrm{H}\boldsymbol{R}^{-1} \tag{14}$$

where the matrix inversion always exists since $\boldsymbol{R}$ is a positive definite Hermitian matrix. With the ZF prerake combining weight, $\boldsymbol{w}^\mathrm{T}\boldsymbol{R}\boldsymbol{\alpha} = \boldsymbol{\alpha}^\mathrm{H}\boldsymbol{\alpha}$, and IPI is completely removed in the received signal.

It is well known that applying a ZF filter to remove the interference in a rake receiver will enhance the additive noise. For prerake combining, since the ZF filtering is done at the transmitter, there is no noise enhancement. However, applying the ZF combining weight $\boldsymbol{w}$ in prerake systems increases the power normalization factor κ, except when $\boldsymbol{R}$ is an identity matrix (no pulse overlapping). This will effectively lower the received SNR as the average transmitted signal power is kept constant.

B. Maximization of the Received SNR Based on Eigenanalysis

Optimum diversity combining in the sense of maximizing the received SNR in a prerake system finds a $\boldsymbol{w}$ that maximizes the output SNR ψ. We assume a quasi-static fading model in which the channel fading coefficients and relative path delays are static over a block of data. Next, we apply the eigenanalysis method to maximize the instantaneous SNR in each block to achieve optimum system performance.

As easily seen from (13), the correlator output SNR of a prerake system in the presence of IPI now becomes $\psi = (E_\mathrm{b}\boldsymbol{w}^\mathrm{T}\boldsymbol{R}\boldsymbol{\alpha}\boldsymbol{\alpha}^\mathrm{H}\boldsymbol{R}^\mathrm{H}\boldsymbol{w}^*)/(\kappa N_0)$. Maximizing ψ is equivalent to maximizing $\psi' = (\boldsymbol{w}^\mathrm{T}\boldsymbol{R}\boldsymbol{\alpha}\boldsymbol{\alpha}^\mathrm{H}\boldsymbol{R}^\mathrm{H}\boldsymbol{w}^*)/(\kappa) = (\boldsymbol{w}^\mathrm{T}\boldsymbol{R}\boldsymbol{\alpha}\boldsymbol{\alpha}^\mathrm{H}\boldsymbol{R}^\mathrm{H}\boldsymbol{w}^*)/(\boldsymbol{w}^\mathrm{T}\boldsymbol{r}\boldsymbol{w}^*)$. From (11), we know that the matrix $\boldsymbol{R}$ is Hermitian and positive definite. By using Cholesky factorization [24], $\boldsymbol{R}$ can be expressed as $\boldsymbol{R} = \boldsymbol{M}^\mathrm{H}\boldsymbol{M}$. If we define a new vector $\boldsymbol{u} = \boldsymbol{M}\boldsymbol{w}^*$, ψ' can be rewritten as $(\boldsymbol{u}^\mathrm{H}\boldsymbol{M}\boldsymbol{\alpha}\boldsymbol{\alpha}^\mathrm{H}\boldsymbol{M}^\mathrm{H}\boldsymbol{u})/(\boldsymbol{u}^\mathrm{H}\boldsymbol{u})$. From the minimax theorem in eigenanalysis [24], the optimum prerake combining vector

$$\boldsymbol{u}_\mathrm{opt} = \arg\max_{\boldsymbol{u}} \left\{ \frac{\boldsymbol{u}^\mathrm{H}\boldsymbol{M}\boldsymbol{\alpha}\boldsymbol{\alpha}^\mathrm{H}\boldsymbol{M}^\mathrm{H}\boldsymbol{u}}{\boldsymbol{u}^\mathrm{H}\boldsymbol{u}} \right\} \tag{15}$$

is the principal eigenvector (the eigenvector corresponding to the largest eigenvalue) of $\boldsymbol{M}\boldsymbol{\alpha}\boldsymbol{\alpha}^\mathrm{H}\boldsymbol{M}^\mathrm{H}$. Because $\boldsymbol{M}\boldsymbol{\alpha}\boldsymbol{\alpha}^\mathrm{H}\boldsymbol{M}^\mathrm{H} = \boldsymbol{M}\boldsymbol{\alpha}(\boldsymbol{M}\boldsymbol{\alpha})^\mathrm{H}$ is formed from a single-column vector $\boldsymbol{M}\boldsymbol{\alpha}$, it is only of rank 1 with only one nonzero eigenvalue corresponding to the principal eigenvector $\boldsymbol{v} = \boldsymbol{M}\boldsymbol{\alpha}$. We let $\boldsymbol{u}_\mathrm{opt} = \boldsymbol{v}$, which apparently leads to the conclusion that $\boldsymbol{w} = \boldsymbol{\alpha}^*$. This implies that, interestingly, even in the presence of IPI, MRC is still the optimum linear prerake diversity combining scheme. This choice of the prerake combining weight results in the same error performance as a conventional rake receiver with MRC when IPI is present.

IV. Performance in the Presence of NBI

A. Signal Model

Prerake and rake systems may perform differently in the presence of NBI. This is because the receiver of a prerake system takes only one sample per bit for detection, whereas the receiver of a rake system needs L_p samples. Let $I(t)$ represent the interference signal. The correlator output for the ith information bit of a prerake system when NBI is present is modified as

$$\begin{aligned}\Delta' &= \sqrt{\frac{E_\mathrm{b}}{\kappa}} b(i)\boldsymbol{w}^\mathrm{T}\boldsymbol{R}\boldsymbol{\alpha} + n' + \Delta_\mathrm{I}' \\ &= \Delta_\mathrm{S}' + \Delta_\mathrm{N}' + \Delta_\mathrm{I}'\end{aligned} \tag{16}$$

where $\Delta_\mathrm{I}' = \int_{-\infty}^{\infty} I(t)p(t - iT_\mathrm{b})dt$, and for the convenience of discussion in the following sections, we have defined Δ_S' and Δ_N' to represent, respectively, the first and second terms of the right-hand side of the equation. The NBI does not change the weight selection process for prerake diversity combining since the instantaneous NBI energy collected by the receiver is independent of the weight vector $\boldsymbol{w}$.

As concluded in Section III, rake and prerake systems with MRC have the same error performance when only AWGN is present. However, the NBI terms in the decision variables of rake and prerake receivers have different distributions, which may result in different error performances for the two schemes. Let us examine the NBI terms in the decision variables for rake and prerake schemes. When NBI is present, the combiner output of a common rake receiver is expressed as

$$\begin{aligned}\Delta =& \sqrt{E_\mathrm{b}} b(i)\boldsymbol{w}^\mathrm{T}\boldsymbol{R}\boldsymbol{\alpha} + \sum_{l=0}^{L_\mathrm{p}-1} w_l n_l + \sum_{l=0}^{L_\mathrm{p}-1} w_l I_l \\ =& \Delta_\mathrm{S} + \Delta_\mathrm{N} + \Delta_\mathrm{I}\end{aligned} \tag{17}$$

where $I_l = \int_{-\infty}^{\infty} I(t)p(t - iT_\mathrm{b} - \tau_l)dt$. Notice the following main difference between the interference term Δ_I in (17) for rake systems and the interference term Δ_I' in (16) for prerake systems: Δ_I' is a single integral, whereas Δ_I is the sum of

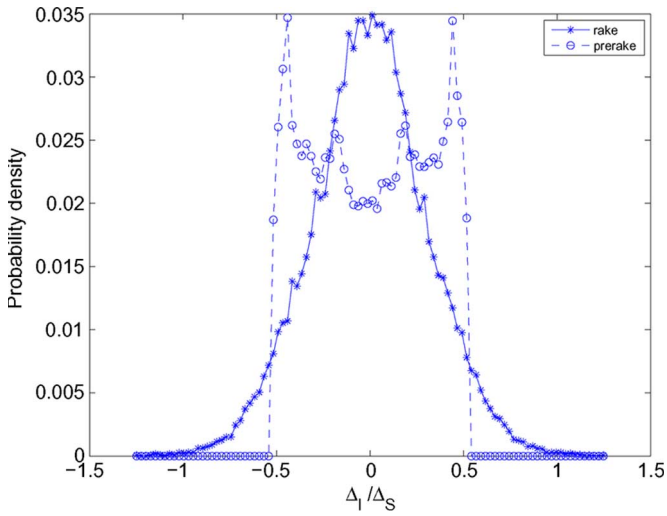

Fig. 2. Distributions of NBI experienced by prerake and rake systems in the presence of in-band tone interferers.

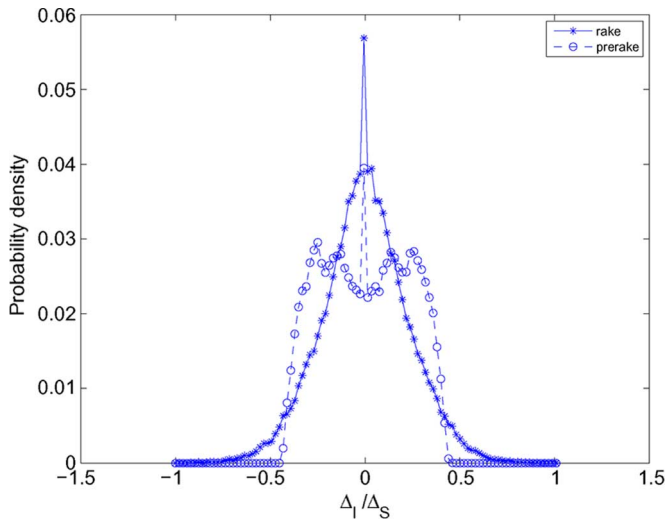

Fig. 3. Distributions of NBI experienced by prerake and rake systems in the presence of in-band-modulated interferers.

L_p terms. To make the comparison fair, fading, AWGN, and NBI experienced by both the rake and prerake systems must be kept the same. For all practical scenarios, the time span of the L_p paths is much shorter than the coherence time of the NBI waveforms. It is thus reasonable to assume that $I_l \approx \Delta_I', l = 0, \ldots, L_p - 1$. For prerake systems, NBI experienced by the receiver only depends on NBI $I(t)$ and UWB pulse shape $p(t)$, as is clearly seen from Δ_I', which is defined in (16). For rake systems, the elements of the multipath combining weight vector $\boldsymbol{\omega}$ (which is equal to $\boldsymbol{\alpha}^*$ if MRC is adopted) are random variables (RVs). Therefore, as clearly seen from (17), besides $I(t)$ and $p(t)$, the distribution of NBI experienced by the receiver also depends on the distribution of $\sum_{l=0}^{L_p-1} \omega_l$.

These differences are illustrated via simulation in which NBI is generated following the specification given in [25] and [26]. We consider the following two types of narrow-band interferers: an in-band tone interferer and an in-band-modulated interferer that uses BPSK modulation and root-raised cosine (RRC) baseband waveform with a bandwidth of 5 MHz and a roll-off factor of 0.25. As we assume a quasi-static multipath fading model for the simulation, the channel varies block by block. Over each block, the NBI signals experienced by the receiver have a random in-band carrier frequency. For simplicity and without loss of generality, the average power of the multipath channel is normalized as $E\{\sum_{l=0}^{L_p-1} |\alpha_l|^2\} = 1$ so that E_b/N_0 is equal to the average received SNR. Fig. 2 shows the distribution of NBI experienced by a rake and a prerake system when a tone interferer is present, while the case with a modulated interferer is shown in Fig. 3. In both cases, the average NBI signal power seen at the receiver is chosen to be 6 dB stronger than the transmitted power of the data signal. The details of the method to generate the data signal will be given in Section V. In both figures, the NBI experienced by the rake and prerake systems exhibits different distribution characteristics, which might lead to different performances of these schemes in the presence of NBI.

In addition, as shown in Figs. 2 and 3, the distributions of NBI with a rake and a prerake receiver for different types of interference (tone and modulated interferers) are similar although not identical. Therefore, in the following analysis, we focus on analyzing the bit error rate (BER) performances of rake and prerake systems in the presence of tone interferers; the conclusions derived from this case should be applicable to predict the relative performances of rake and prerake schemes in the presence of modulated NBI. This will be further validated via simulation.

The analysis becomes extremely complex when pulse overlapping is considered; thus, we will focus on the case that received pulses that do not overlap in the theoretical analysis of the relative performances of rake and prerake schemes in the presence of NBI and resort to simulation for more general scenarios. Nevertheless, the results derived based on such simplification could serve as a BER lower bound. Without loss of generality, we assume that the ith transmitted bit is a "1" and derive the conditional BER.[2]

For rake systems with a perfect path resolution (no IPI) and MRC and $b(i) = 1$, the two terms Δ_S and Δ_I given in (17) are simplified as

$$\Delta_S = \sqrt{E_b} \sum_{l=0}^{L_p-1} \alpha_l^2 = \theta\sqrt{E_b} \tag{18a}$$

$$\Delta_I = \sum_{l=0}^{L_p-1} \alpha_l I_l \tag{18b}$$

where $\theta = \sum_{l=0}^{L_p-1} \alpha_l^2$.

Similarly, for prerake systems, the Δ_S' given in (16) is simplified as

$$\Delta_S' = \sqrt{E_b \sum_{l=0}^{L_p-1} \alpha_l^2} = \sqrt{E_b\theta}. \tag{19}$$

[2]When input bits have an equal probability to take on the value of "1" and "−1," which is assumed to be the case in this paper, the conditional BER is equal to the average BER.

B. Distribution of Δ_{I} and Δ'_{I}

The system performance with in-band tone interferers will be bounded by the following two extreme cases: with one tone interferer and with a large number of tone interferers. Thus, we will analyze the performances of rake and prerake schemes for these two cases next.

1) Single Tone Interferer: For prerake schemes, when there is only one in-band tone interferer, the interference component Δ'_{I} at the output of the prerake receiver can be viewed as samples at the receiver filter output whose input is a sinusoidal signal. Since the filter is matched to the ultrashort UWB pulse, the interference at the filter output is effectively a sampled sinusoidal signal in which the sampling time has a uniform distribution. Therefore, Δ'_{I} at the output of the filter has a harmonic distribution given by [21]

$$p_{\Delta'_{\mathrm{I}}}(x) = \begin{cases} \frac{1}{\pi\sqrt{2\sigma_{\mathrm{I}}^2 - x^2}}, & |x| < \sqrt{2}\sigma_{\mathrm{I}} \\ 0, & \text{otherwise} \end{cases} \tag{20}$$

where σ_{I}^2 is the variance of the tone interferer, which corresponds to the average power of the interferer if the filter energy is normalized to unity.

For rake schemes, the NBI component at the receiver output is a sum of multiple interference terms, each scaled by a combining weight coefficient, as expressed in Δ_{I}. Since all combining weight coefficients are independent and almost identically distributed RVs in the case of MRC, this sum may be approximated as a Gaussian RV when the number of rake fingers is large.

2) Multiple Tone Interferers: For prerake schemes, when multiple tone interferers of different frequencies are present simultaneously, the contributions to Δ'_{I} from each sinusoidal signals can be considered as independent RVs with a harmonic distribution. As the number of interferers becomes large, the NBI distribution can be approximated as Gaussian by invoking the central limit theorem. Note that there could be cases when the number of tone interferers is not large enough but greater than one in which neither a harmonic distribution nor a Gaussian distribution is an accurate approximation.

For rake schemes, Δ_{I} contains even more terms than the case with one tone interferer. Thus, the same reason as given for the case of a single tone interferer applies, and Δ_{I} can be approximated as a Gaussian RV.

C. Distribution of θ

We apply the UWB indoor channel model in [11]. In the absence of pulse overlapping, the received sample gain θ can be simplified to $\theta = \sum_{l=0}^{L_{\mathrm{p}}-1} \alpha_l^2$, which is a sum of squared multipath fading coefficients that are independent lognormal RVs. To evaluate the probability density function (pdf) of θ, one needs to find the pdf of the sum of independent lognormal RVs. Although an exact closed-form expression does not exist, there are a number of methods to approximate this pdf. We will apply Wilkinson's method [27] to approximate the desired pdf of θ.

As mentioned in Section II-A, the channel coefficient α_l can be modeled as $\alpha_l = \lambda_l \beta_l$, where $\lambda_l \in \{1, -1\}$, and $\beta_l = |\alpha_l|$ is a lognormal RV. Let $\beta_l = |\alpha_l| = e^{u_l}$, where u_l is a normal RV obeying $u_l \sim \mathcal{N}(\mu_{u_l}, \sigma_{u_l}^2)$, and $\theta_l = \alpha_l^2 = e^{2u_l}$. The kth moment of the lognormal variable β_l is then given by

$$E\left\{\beta_l^k\right\} = e^{k\mu_{u_l} + k^2\sigma_{u_l}^2/2}. \tag{21}$$

Let $\theta = \sum_{l=0}^{L_{\mathrm{p}}-1} \theta_l$ be modeled as a lognormal RV, which implies that $\theta = e^x$ and $x \sim \mathcal{N}(\mu_x, \sigma_x^2)$ is a normal RV. In Wilkinson's method, the two parameters μ_x and σ_x can be obtained by matching the first two moments of θ with the first two moments of $\sum_{l=0}^{L_{\mathrm{p}}-1} \theta_l$. Algebraic manipulations lead to the mean $\mu_x = \ln(E_{L1}^2/\sqrt{E_{L2}})$ and the standard deviation $\sigma_x = \sqrt{\ln(E_{L2}/E_{L1}^2)}$, where the two scalars E_{L1} and E_{L2} are related to μ_{u_l} and $\sigma_{u_l}^2$ by

$$E_{L1} = \sum_{l=0}^{L_{\mathrm{p}}-1} e^{\left(2\mu_{u_l} + 2\sigma_{u_l}^2\right)} \tag{22a}$$

$$E_{L2} = \sum_{l=0}^{L_{\mathrm{p}}-1} e^{\left(4\mu_{u_l} + 8\sigma_{u_l}^2\right)} + 2\sum_{l=1}^{L_{\mathrm{p}}-1}\sum_{m=0}^{l-1} e^{2\left(\mu_{u_l} + \mu_{u_m} + \sigma_{u_l}^2 + \sigma_{u_m}^2\right)}. \tag{22b}$$

Put all together, the pdf of θ is approximated as

$$f(\theta) = \frac{1}{\theta\sqrt{2\pi\sigma_x^2}} \exp\left[-\frac{(\ln(\theta) - \mu_x)^2}{2\sigma_x^2}\right]. \tag{23}$$

In the case when an analytical expression of $f(\theta)$ is impossible, the pdf could be obtained via the Monte Carlo simulation, which incorporates the actual channel statistics.

D. Error Probability in the Presence of NBI

When the error rate is dominated by the additive noise component, the analysis becomes simple, and, as explained in Section III, both rake and prerake systems have the same error performance. It will be more interesting to find out how rake and prerake schemes perform in NBI-dominated scenarios. In such a case, we can ignore the additive noise component in the analysis for simplicity. When NBI and AWGN are comparable, their impacts can be separately analyzed (because NBI and AWGN are independent) and then combined to predict the system performance.

1) With One Tone Interferer: The probability of error when multipath fading is absent had been derived in [21]; we extend such results to the case with multipath fading and derive a BER expression conditioned on θ. Assuming binary PAM in which the input takes on the values of "1" and "-1" with

equal probability, we obtain the probability of error conditioned on θ as

$$P(\theta) = \int_{\sqrt{E_b\theta}}^{+\infty} p_{\Delta_I'}(x)dx = \int_{\sqrt{E_b\theta}}^{\sqrt{2}\sigma_I} p_{\Delta_I'}(x)dx. \quad (24)$$

The integral above can be carried out, and (24) can be obtained to be

$$P(\theta) = \begin{cases} \frac{1}{2} - \frac{1}{\pi}\arcsin\left(\sqrt{\frac{\gamma_d}{2}}\right), & \gamma_d < 2 \\ 0, & \gamma_d > 2 \end{cases} \quad (25)$$

where

$$\gamma_d = \frac{\theta E_b}{\sigma_I^2}. \quad (26)$$

2) With Multiple Tone Interferers: When the interference is approximated as Gaussian, the BER expressions conditioned on θ for rake and prerake receivers with binary PAM are expressed as

$$P_{\text{prerake}}(\theta) = \frac{1}{\sqrt{2\pi\sigma_I^2}} \int_{-\infty}^{0} \exp\left[-\frac{(\lambda - \sqrt{E_b\theta})^2}{2\sigma_I^2}\right] d\lambda$$
$$= Q\left(\frac{\sqrt{E_b\theta}}{\sigma_I}\right) \quad (27)$$

$$P_{\text{rake}}(\theta) = \frac{1}{\sqrt{2\pi\sigma_{\Delta_I}^2}} \int_{-\infty}^{0} \exp\left[-\frac{(\lambda - \Delta_s)^2}{2\sigma_{\Delta_I}^2}\right] d\lambda$$
$$= Q\left(\frac{\Delta_s}{\sigma_{\Delta_I}}\right). \quad (28)$$

Recall from (18a) and (18b) that $\Delta_s = \sqrt{E_b\theta}$ and $\sigma_{\Delta_I}^2 = \theta\sigma_I^2$. We thus have

$$P_{\text{rake}}(\theta) = Q\left(\frac{\sqrt{E_b\theta}}{\sigma_I}\right) = P_{\text{prerake}}(\theta). \quad (29)$$

The average BER can be calculated by averaging the conditional BER $P(\theta)$ over the pdf $f(\theta)$ as

$$P_e = \int_0^{\infty} P(\theta) f(\theta) d\theta \quad (30)$$

where $P(\theta)$ has been given in (25) or (29), and $f(\theta)$ has been given in (23).

V. Simulation Results and Discussion

In obtaining simulation results, a carrier-modulated truncated RRC pulse with a roll-off factor of 0.25 is applied as the UWB pulse shape $p(t)$. This pulse has a width of $T_p = 1$ ns and a 10-dB bandwidth of 2 GHz. The system data rate is set as 50 Mb/s. We adopt the CM3 channel model [11] with a root-mean-square delay spread of 15 ns, an average cluster arrival rate of 0.0667/ns, and an average path arrival rate of 2/ns. The cluster decay factor applied is $\Gamma = 14$ ns, the ray decay factor applied is $\gamma = 7.9$ ns, and the standard deviation of the fading coefficients chosen is 3.4 dB. The number of fingers is chosen to be $L_p = 5$, which is a typical choice for many practical systems to provide a balanced complexity and performance. The receiver has perfect knowledge of the channel coefficients and delays.

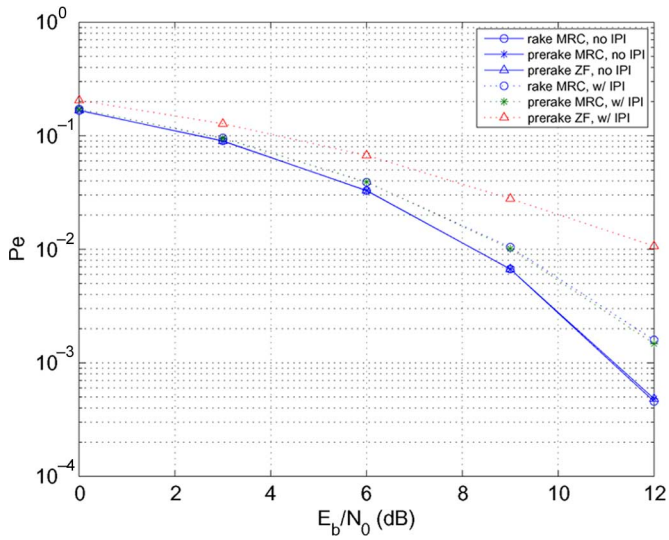

Fig. 4. Simulated BER versus E_b/N_0 curves of the prerake and rake systems with and without IPI (no NBI).

Fig. 4 shows the simulated error performances of prerake and rake systems in the absence of NBI. For comparison, error performances of these systems with and without IPI are provided. All parameters of the channel and the transmitted signals are the same, except that the path arrival rate for the latter case is fixed so that no IPI occurs. It is observed that, although IPI degrades the performance, both prerake and rake systems with MRC perform the same. When there is no pulse overlapping, the ZF scheme for prerake systems is found to have the same performance as MRC rake systems. In the presence of pulse overlapping, however, the ZF optimization for prerake multipath combining performs worse than the MRC scheme for reasons explained in Section III. Although ZF for prerake combining does not enhance noise in the receiver, it requires a higher transmit signal energy per symbol to overcome IPI.

Error performance in the presence of tone NBI is shown in Fig. 5, where the BER values are obtained as a function of the power ratio of the interferers to the transmitted signals. It is observed that, with a single NBI source, the prerake scheme performs several decibels better than the conventional rake scheme at the low-BER region. This is due to the different distributions of the interference the rake and prerake receivers experienced. It also validated the conclusion made in Section IV-B that the prerake scheme tends to perform the same as the rake scheme as the number of independent interferers increases. The analytical curves obtained by applying the harmonic-distributed and Gaussian-approximated NBI given in Section IV match very well with the simulated curves for both rake and prerake systems for the single-interferer scenario. The analytical curve

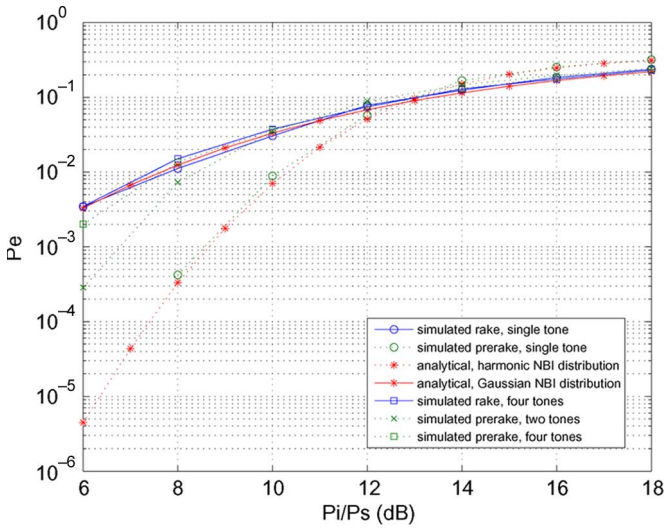

Fig. 5. Analytical and simulated BER versus P_i/P_s curves of the prerake and rake systems with tone interferers.

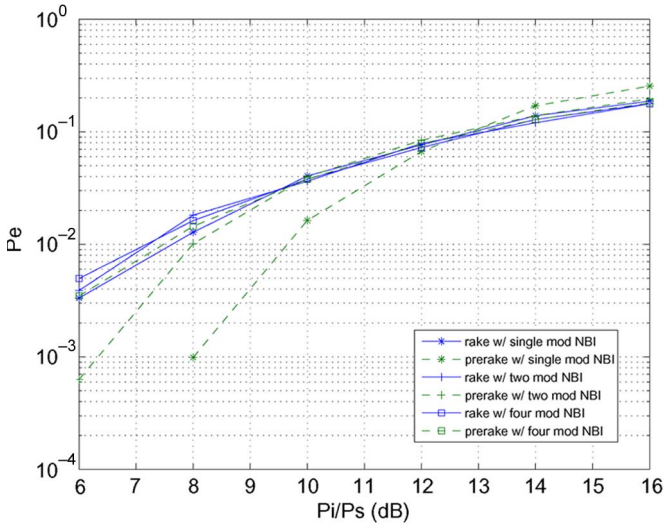

Fig. 6. Simulated BER versus P_i/P_s curves of the prerake and rake systems with modulated interferers.

with Gaussian-distributed NBI can also serve as an upper bound for prerake systems with multiple interferers.

Fig. 6 shows the simulated BER curves in the presence of in-band-modulated interferers. The NBI signals are generated using the method and parameters described in Section IV-A and at the beginning of this section. To clearly assess the different behaviors of rake and prerake schemes in the presence of NBI, AWGN and IPI are not considered in Figs. 5 and 6. Note that we have assumed perfect channel estimation for both types of receivers. How NBI affects the channel-estimation quality of rake and prerake systems is a complex issue and is beyond the scope of this paper.

VI. Conclusion

We have optimized the prerake multipath combining scheme for pulsed UWB in the presence of IPI caused by pulse overlapping. MRC is still proved to be the optimum linear multipath combining scheme for prerake systems in the sense of maximum received SNR when the system is distorted by AWGN and IPI. We have also assessed the receiver behavior and the error performance of both the prerake and the conventional rake schemes in the presence of NBI. In the absence of NBI, both the rake and prerake schemes with the same set of combining weights have identical performances. When the number of NBI signals is small in which the interference components in the receiver cannot be approximated as Gaussian, however, the prerake scheme has been found to outperform the rake scheme. The performance gap between rake and prerake schemes reduces as the number of NBI sources increases.

References

[1] R. V. Nee and R. Prasad, *OFDM for Wireless Multimedia Communications*. Norwood, MA: Artech House, 2000.

[2] J. Balakrishnan, A. Batra, and A. Dabak, "A multi-band OFDM system for UWB communication," in *Proc. UWBST*, Nov. 2003, pp. 354–358.

[3] *UWB Communications Systems: A Comprehensive Overview*, M. G. diBenedetto, T. Kaiser, A. F. Molisch, I. Oppermann, C. Politano, and D. Porcino, Eds. New York: Hindawi, 2005.

[4] M. Z. Win and R. A. Scholtz, "Impulse radio: How it works," *IEEE Commun. Lett.*, vol. 2, no. 2, pp. 36–38, Feb. 1998.

[5] R. Qiu, H. Liu, and X. S. Shen, "Ultra-wideband for multiple-access communications," *IEEE Commun. Mag.*, vol. 43, no. 2, pp. 80–87, Feb. 2005.

[6] H. Liu, "Error performance of a pulse amplitude and position modulated ultra-wideband system in lognormal fading channels," *IEEE Commun. Lett.*, vol. 7, no. 11, pp. 531–533, Nov. 2003.

[7] M. Z. Win and R. A. Scholtz, "On the energy capture of ultrawide bandwidth signals in dense multipath environments," *IEEE Commun. Lett.*, vol. 2, no. 9, pp. 245–247, Sep. 1998.

[8] S. Gaur and A. Annamalai, "Improving the range of UWB transmission using RAKE receivers," in *Proc. 53rd IEEE VTC*, Oct. 2003, vol. 1, pp. 597–601.

[9] R. Esmailzadeh, E. Sourour, and M. Nakagawa, "Prerake diversity combining in time-division duplex CDMA mobile communications," *IEEE Trans. Veh. Technol.*, vol. 48, no. 3, pp. 795–801, May 1999.

[10] K. Usuda, H. Zhang, and M. Nakagawa, "Pre-Rake performance for pulse based UWB system in a standardized UWB short-range channel," in *Proc. IEEE WCNC*, Mar. 2004, vol. 2, pp. 920–925.

[11] A. F. Molisch, J. R. Foerster, and M. Pendergrass, "Channel models for ultrawideband personal area networks," *Wireless Commun.*, vol. 10, no. 6, pp. 14–21, Dec. 2003.

[12] A. F. Molisch, K. Balakrishnan, C. C. Chong, D. Cassioli, S. Emami, A. Fort, J. Karedal, J. Kunisch, H. Schantz, and K. Siwiak, "A comprehensive model for ultrawideband propagation channels," *IEEE Trans. Antennas Propag.*, vol. 54, pt. 1, no. 11, pp. 3151–3166, Nov. 2006.

[13] M. Hamalainen, V. Hovinen, R. Tesi, J. H. J. Iinatti, and M. Latva-aho, "On the UWB system coexistence with GSM900, UMTS/WCDMA, and GPS," *IEEE J. Sel. Areas Commun.*, vol. 20, no. 9, pp. 1712–1721, Dec. 2002.

[14] Z. Xu, B. Sadler, and J. Tang, "Data detection for UWB transmitted reference systems with inter-pulse interference," in *Proc. IEEE ICASSP*, Mar. 2005, pp. 601–604.

[15] S. Zhao and H. Liu, "On the optimum linear receiver for impulse radio system in the presence of pulse overlapping," *IEEE Commun. Lett.*, vol. 9, no. 4, pp. 340–342, Apr. 2005.

[16] X. Chu and R. Murch, "Performance analysis of DS-MA impulse radio communications incorporating channel-induced pulse overlap," *IEEE Trans. Wireless Commun.*, vol. 5, no. 4, pp. 948–959, Apr. 2006.

[17] L. Zhao and A. M. Haimovich, "Performance of ultra-wideband communications in the presence of interference," *IEEE J. Sel. Areas Commun.*, vol. 20, no. 9, pp. 1684–1691, Dec. 2002.

[18] J. R. Foerster, "The performance of a direct-sequence spread ultra-wideband system in the presence of multipath, narrowband interference and multiuser interference," in *Proc. IEEE UWBST*, 2002, pp. 87–91.

[19] T. Strohmer, M. Emami, J. Hansen, G. Papanicolaou, and A. J. Paulraj, "Application of time-reversal with MMSE equalizer to UWB communications," in *Proc. IEEE GLOBECOM*, Nov. 2004, pp. 3123–3127.

[20] M. B. Donlan, S. Venkatesh, V. Bharadwaj, M. R. Buehrer, and J.-A. Tsai, "The ultra-wideband indoor channel," in *Proc. IEEE VTC—Spring*, May 2004, pp. 208–212.
[21] L. Piazzo and F. Ameli, "Performance analysis for impulse radio and direct-sequence impulse radio in narrowband interference," *IEEE Trans. Commun.*, vol. 53, no. 9, pp. 1571–1580, Sep. 2005.
[22] Z. Tian, L. Yang, and G. B. Giannakis, "Symbol timing estimation in ultra wideband communications," in *Proc. 36th IEEE Asilomar Conf. Signals, Syst., Comput.*, Nov. 2002, pp. 1924–1928.
[23] I. Guvenc and H. Arslan, "Performance evaluation of UWB systems in the presence of timing jitter," in *Proc. IEEE UWBST*, Nov. 2003, pp. 136–141.
[24] S. Haykin, *Adaptive Filter Theory*, 4th ed. Englewood Cliffs, NJ: Prentice-Hall, 1996.
[25] *IEEE P802.15.3a alternative PHY selection criteria*, Dec. 2002. IEEE 802.15.3a Tech. Eds., Document IEEE P802.15-03/031r5.
[26] *IEEE P802.15.4a alternative PHY selection criteria*, Nov. 2004. IEEE 802.15.4a Tech. Eds., Document IEEE P802.15-04-0232-16-004a.
[27] N. C. Beaulieu, A. A. Abu-Dayya, and P. J. Mclane, "Estimating the distribution of a sum of independent lognormal random variable," *IEEE Trans. Commun.*, vol. 43, no. 12, pp. 2869–2873, Dec. 1995.

Shiwei Zhao received the B.S. degree in computer science from the University of Science and Technology of China, Hefei, China, in 1999, and the Ph.D. degree in electrical engineering from Oregon State University, Corvallis, in 2006.

From January 2005 to June 2005, he conducted research with Mitsubishi Electric Research Laboratories, Cambridge, MA, with a focus on drafting proposals to the IEEE 802.15.4a study group (low-rate ultrawideband (UWB) systems). Since June 2006, he has been a Wireless Systems Engineer with Trapeze Networks, Pleasanton, CA, where he is working on RF management. He has published many journal and conference papers in the area of UWB communications and has filed three patent applications.

Huaping Liu (S'95–M'97) received the B.S. and M.S. degrees in electrical engineering from Nanjing University of Posts and Telecommunications, Nanjing, China, in 1987 and 1990, respectively, and the Ph.D. degree in electrical engineering from the New Jersey Institute of Technology, Newark, in 1997.

From July 1997 to August 2001, he was with Lucent Technologies, Murray Hill, NJ. Since September 2001, he has been with the School of Electrical Engineering and Computer Science, Oregon State University, Corvallis, where he is currently an Associate Professor. His research interests include capacity and performance analysis of wireless networks, communication techniques for multiuser time-varying environments with applications to cellular and indoor wireless communications, ultrawideband schemes, and multiple-input multiple-output orthogonal-frequency-division-multiplexing systems.